0026-895X/93/010093-09$03.00/0

MOLECULAR PHARMACOLOGY, 44:93-101

Expression of the Pore-Forming P_{2z} Purinoreceptor in *Xenopus* Oocytes Injected with Poly(A)$^+$ RNA from Murine Macrophages

LOUISE C. NUTTLE, CHAKIB EL-MOATASSIM, and GEORGE R. DUBYAK

Department of Physiology and Biophysics, School of Medicine, Case Western Reserve University, Cleveland, Ohio 44106

Received January 13, 1993; Accepted April 7, 1993

SUMMARY

Extracellular ATP activates two distinct types of P_2 purinoreceptor-mediated signaling pathways in macrophages, 1) the rapid formation of nonselective pores/channels in the plasma membrane and 2) a guanine nucleotide-binding protein-dependent stimulation of phosphotidylinositol-specific phospholipase C, with subsequent mobilization of intracellular Ca^{2+}. Several studies have suggested that the pore-forming, or P_{2z}, purinoreceptor may be involved in the cytolytic effects of ATP on macrophages and other cell types. We have identified 3′-*O*-(4-benzoyl)benzoyl-ATP (BzATP) and UTP as selective agonists for the P_{2z} purinoreceptor and Ca^{2+}-mobilizing nucleotide receptor, respectively, in BAC1.2F5 macrophages. In this paper we demonstrate that BzATP and ATP (but not UTP) activate membrane depolarization in BAC1.2F5 cells and also stimulate appropriate electrophysiological responses, consistent with the expression of the P_{2z} purinoreceptor, in *Xenopus* oocytes injected with poly(A)$^+$ RNA derived from BAC1.2F5 cells. Micromolar concentrations of BzATP or millimolar concentrations of ATP induced a sustained increase in the membrane holding current in these voltage-clamped oocytes. This response was significantly potentiated in the absence of extracellular divalent cations, consistent with the specificity of the P_{2z} purinoreceptor for tetrabasic nucleotides. The sustained currents induced by BzATP or ATP were distinct from the transient and/or oscillating increases in Ca^{2+}-dependent Cl^- currents that were stimulated by UTP but not BzATP. UTP-stimulated transient currents and nucleotide-dependent increases in aequorin luminescence in poly(A)$^+$ RNA-injected oocytes were independent of extracellular Ca^{2+} and were correlated with the mobilization of intracellular Ca^{2+} stores. Sucrose fractionation of the poly(A)$^+$ RNA from BAC1.2F5 cells resulted in the enrichment of mRNA species encoding the components of the P_{2z} purinoreceptor, as well as the Ca^{2+}-mobilizing nucleotide receptor, in fractions containing 2.5–4.0-kilobase species.

Extracellular ATP (and other nucleotides) can activate a variety of cellular responses via the occupation of a class of cell surface receptors that have been termed P_2 purinoreceptors (for reviews, see Refs. 1–3). In general, the effects of extracellular nucleotides acting through distinct P_2 purinoreceptors can be grouped into three classes, 1) the G protein-mediated activation of phosphotidylinositol-specific phospholipase C, with subsequent mobilization of inositol trisphosphate-releasable Ca^{2+} stores (via P_{2y} and ATP/UTP receptor subtypes), 2) the activation of cation channels (via the P_{2x} receptor subtype), and 3) the reversible formation of nonselective pores (via the P_{2z} receptor subtype).

ATP-induced permeabilization has been described in a number of cells including macrophages (4–6), transformed mouse fibroblasts (7), mast cells (8, 9), certain subtypes of lymphocytes (10, 11), hemopoietic stem cells (12), and neuroblastoma cells (13). The permeabilizing effect of ATP is dependent on the concentration of ATP^{4-} (9, 14) and is enhanced in the absence of divalent cations, by increased extracellular pH (15), and by depletion of intracellular ATP (16). ATP-induced permeabilization can be reversed by the direct removal of ATP^{4-} or by the addition of Mg^{2+} to form Mg-ATP complexes (17). The mechanism of ATP-induced pore formation, however, has not yet been determined.

Activation of P_{2z} purinoreceptors exerts many effects on macrophage function, including increases in Na^+ influx, K^+ efflux, and $[Ca^{2+}]_i$, inhibition of phagocytosis, membrane depolarization (4), and an increased permeability to molecules of ≤900 Da (5). Sustained occupation of these receptors can result in cytolysis (18). The lytic effects of ATP on human macrophages become irreversible after a short "trigger" exposure, indicative of a programmed cell lysis. A similar effect is found in thymocytes and certain tumor cell lines in which ATP

This work was supported in part by Grant GM36387 from the National Institutes of Health and Grant 91012060 from the American Heart Association. G.R.D. is an Established Investigator of the American Heart Association. C.E.-M. is supported in part by a Philippe Foundation Award. L.C.N. is supported in part by a Cleveland Cardiovascular Training Grant (HL07653) from the National Institutes of Health.

ABBREVIATIONS: G protein, guanine nucleotide-binding protein; SKR, substance K receptor; BSS, balanced salt solution; DEPC, diethylpyrocarbonate; MBS, modified Barth's saline; $[Ca^{2+}]_i$, intracellular Ca^{2+} concentration; BzATP, 3′-*O*-(4-benzoyl)benzoyl-ATP; ATP[S], adenosine-5′-*O*-(3-thio)triphosphate; GTP[S], guanosine-5′-*O*-(3-thio)triphosphate; HEPES, 4-(2-hydroxyethyl)-1-piperazineethanesulfonic acid; EGTA, ethylene glycol bis(β-aminoethyl ether)-*N*,*N*,*N*′,*N*′-tetraacetic acid.

triggers apoptosis, or programmed cell death (19). In these cells, ATP-induced apoptosis is dependent on the concentration of ATP^{4-} and, as in macrophages, is selective for ATP, consistent with the specific involvement of the pore-forming P_{2z} purinoreceptor. Pore formation alone, however, is insufficient for the activation of apoptosis, because perforin cannot mimic the effect of ATP. The implication of cooperative effects of pore formation and ATP-induced responses is particularly intriguing in light of recent evidence that occupation of the P_{2z} purinoreceptor leads to the activation of phospholipase D, as well as permeabilization, in murine macrophages (20). These parallel effects of ATP acting through the P_{2z} purinoreceptor suggest an important, but ill defined, role for this receptor in macrophage function.

Steinberg and Di Virgilio (21) have suggested that ATP may be an important intercellular signal during cell-cell contact. T lymphocytes have been shown to release ATP in response to T cell antigen receptor cross-linking (22). ATP released into the restricted space between T cells and their targets may play a role in the killing of target cells and/or the interaction of T cells with antigen-presenting macrophages and B cells. The rapid degradation of ATP by ectonucleotidases and the inhibitory effects of divalent cations have been suggested as two mechanisms by which the localized effects of ATP could be terminated after dissociation of the cytolytic T lymphocyte and target cell (21). Significantly, the sensitivity of human macrophages to ATP-induced lysis is enhanced by treatment with the cytokine interferon-γ. The up-regulation of ATP sensitivity may provide a mechanism by which activated macrophages are selectively targeted for removal by cytolytic T lymphocytes (18).

Due to the lack of specific ligands, no ATP receptor has been isolated to date. Several receptor ion channels and G protein-coupled receptors have been functionally expressed, characterized, and cloned using the *Xenopus* oocyte expression system. Two groups have independently described the expression of Ca^{2+}-mobilizing P_2 purinoreceptors in *Xenopus* oocytes injected with either mRNA from HL-60 granulocytes (23) or mRNA from embryonic guinea pig brain (24). In contrast, the P_{2z} purinoreceptor is functionally similar to receptor ion channels and thus may exist as an oligomeric membrane protein. We previously confirmed the expression of this receptor in the BAC1.2F5 murine macrophage cell line (20). In this paper we describe for the first time the functional expression of an exogenous pore-forming P_{2z} purinoreceptor in *Xenopus* oocytes, a cell type that does not normally express this receptor.

Experimental Procedures

Materials. Collagenase type IA, 3-aminobenzoic acid ethyl ether, DEPC, and all nucleotides, with the exception of ATP[S], were from Sigma Chemical Co. ATP[S] and oligo(dT)-cellulose were purchased from Boehringer Mannheim. Platelet-activating factor (1-*O*-stearyl-2-acetyl-*sn*-glycero-3-phosphocholine) was from Calbiochem. Methylmercuric hydroxide was from Alfa Products. Fura-2 and bis-oxonol were from Molecular Probes, Inc. The SKR cDNA clone was kindly provided by Shigetada Nakanishi (Kyoto University, Japan). BAC1.2F5 cells were a gift from Richard Stanley (Albert Einstein College of Medicine).

Cell culture. The BAC1.2F5 cell line is a clone of the SV40-transformed murine macrophage cell line BAC1, which is completely dependent on colony-stimulating factor-1 for survival and growth. BAC1.2F5 cells were routinely cultured in Dulbecco's modified essential medium supplemented with 15% fetal calf serum (Hyclone), 25% L cell-conditioned medium as a source of colony-stimulating factor-1, 50 units/ml penicillin, and 50 μg/ml streptomycin, in a humidified atmosphere of 95% air/5% CO_2. The cells were seeded in 100- × 20-mm tissue culture dishes and grown to 80–90% confluence for 3–4 days. Adherent cells were washed once with Ca^{2+}/Mg^{2+}-free Hanks' BSS and starved in L cell-conditioned medium-free culture medium for 15–18 hr before an experiment.

$[Ca^{2+}]_i$ measurements. $[Ca^{2+}]_i$ was measured in BAC1.2F5 cells using the fluorescent indicator fura-2 as described previously (20), with the following modifications. Cells were concentrated to 4×10^6 cells/ml in Ca^{2+}-containing BSS (125 mM NaCl, 5 mM KCl, 1 mM $MgCl_2$, 1.5 mM $CaCl_2$, 25 mM HEPES, pH 7.5), supplemented with 0.1% bovine serum albumin and 5 mM glucose, before measurements. Concentrated cells (0.25 ml) were diluted to 5×10^5 cells/ml with 1.75 ml of Ca^{2+}-free BSS. EGTA (375 μM) was added to chelate residual Ca^{2+}, followed immediately by the nucleotide, in an effort to minimize depletion of intracellular stores. Maximal fluorescence was determined upon the addition of 2 mM $CaCl_2$ and 50 ng/μl digitonin.

Membrane potential measurements. Quiescent BAC1.2F5 cells were harvested by scraping in Ca^{2+}-free BSS, washed twice, and resuspended at 2×10^6 cells/ml in BSS supplemented with 5 mM glucose, with or without divalent cations as indicated. Cell suspensions were stored for up to 3 hr on ice before measurements. The cell suspension (0.5 ml) was diluted to a final concentration of 5×10^5 cells/ml with 1.5 ml of buffer. Bis-oxonol was added to 200 nM and its fluorescence was monitored (540-nm excitation/580-nm emission) as described (25).

Poly(A)$^+$ RNA isolation and fractionation. RNA was isolated using the acid-guanidinium thiocyanate-phenol-chloroform extraction method, as described by Chomczynski and Sacchi (26). Total RNA was poly(A)$^+$ selected using oligo(dT)-cellulose chromatography. BAC1.2F5 poly(A)$^+$ RNA (500 μg) from three separate preparations was dissolved in 10 mM Tris·HCl, pH 7.6, 10 mM NaCl, 1 mM EDTA (TNE), that had been treated with 0.1% DEPC. The sample was heated to 65° for 10 min and chilled on ice. Methylmercuric hydroxide was added to a final concentration of 20 mM and the sample was immediately layered on a 5–25% sucrose gradient prepared in DEPC-treated TNE. Fractionation was acheived by centrifugation at 27,000 rpm for 16 hr in a SW28.1 rotor (Beckman). Thirty 400-μl fractions were collected and treated with 2.5 mM 2-mercaptoethanol. Aliquots of each fraction were removed for spectrophotometric quantitation. The remaining samples were precipitated with ethanol and dissolved in DEPC-treated water to 1 μg/μl. Individual fractions were pooled into six groups of five fractions each. Distribution of the RNA through the gradient was determined by electrophoresis of several individual fractions through a 1% agarose-2% formaldehyde gel, alongside an RNA standard ladder (Bethesda Research Laboratories).

Oocyte isolation and injection. Adult female *Xenopus laevis* (Nasco) were anesthetized with 0.2% 3-aminobenzoic acid ethyl ether. Ovarian lobes were surgically removed, washed, and incubated for 30 min in Ca^{2+}-free MBS (15 mM HEPES, 88.0 mM NaCl, 1.0 mM KCl, 2.4 mM $NaHCO_3$, 1.5 mM $MgSO_4$) containing 1.5 mg/ml collagenase type IA. The oocytes were then washed extensively in MBS (same as described above but containing 0.41 mM $CaCl_2$, 0.3 mM $CaNO_3$, and 0.82 mM $MgSO_4$), manually separated, and maintained at 18–20° in MBS supplemented with 2.5 mM pyruvate, 50 units/ml penicillin, and 50 μg/ml streptomycin or with 2.5 mM pyruvate, 50 μg/ml gentamicin, and 0.5 mM theophylline. (No functional differences were observed using these medium compositions.) After 1 day of recovery, oocytes were injected equatorially with 50 nl of DEPC-treated water, poly(A)$^+$ RNA (1 μg/μl), or purified SKR mRNA (10 ng/μl) transcribed from the cloned SKR cDNA, as a positive translational control. Injections were performed using a WPI pneumatic picopump (PV 820) and glass pipettes pulled to a tip diameter of 5–7 μm.

Electrophysiology. Oocytes were impaled with two glass electrodes containing 3 M KCl and were clamped at a membrane potential of −60 mV while being bathed in 1 ml of MBS (with or without divalent cations as indicated), using an Axoclamp 2A amplifier (Axon Instruments). Additions were made by removing 200 μl of the bath solution

and adding back 200 μl of 5-fold concentrated agonist in the indicated bath solution.

Aequorin measurements. Oocytes were injected with 25 nl of aequorin (2 mg/ml stock solution with 20 μM EGTA) and incubated for 3 hr before measurements. Aequorin luminescence was recorded from individual oocytes, in relative light units integrated over 20-sec periods, using a Lumat LB 9501 luminometer (Berthold). Basal luminescence was measured for 1 min in 80 μl of MBS (0 Ca^{2+}, 0.8 mM Mg^{2+}). Agonists were added from 5-fold concentrated stock solutions in the same buffer.

Data analysis. Data were subjected to nonlinear regression analysis using InPlot software. For all curves, r^2 values were >0.993.

Results

Extracellular nucleotides activate membrane depolarization and Ca^{2+} mobilization in BAC1.2F5 macrophages. The characteristics of the P_{2z} purinoreceptor and the ATP/UTP, or nucleotide, receptor are summarized in Table 1. The occupancy of the P_{2z} purinoreceptor activates transmembrane ion fluxes that result in the collapse of ion gradients and membrane depolarization. In these studies we used membrane depolarization as an index of P_{2z} purinoreceptor-induced pore formation. BzATP and UTP were used as selective agonists for the the pore-forming P_{2z} purinoreceptor and Ca^{2+}-mobilizing receptor, respectively (20). In the presence of bis-oxonol, a membrane potential-sensitive dye, BAC1.2F5 macrophages displayed a concentration-dependent depolarization when stimulated with BzATP (Fig. 1A) or ATP (Fig. 1B). Both the kinetics and magnitude of membrane depolarization were dependent on the concentration of BzATP or ATP. Nucleotide dose-response curves for the depolarizing effects of BzATP and ATP in BAC1.2F5 cells (Fig. 2A) showed a half-maximal effective concentration (EC_{50}) for BzATP of 0.1 mM. ATP was less potent, with an estimated EC_{50} of 0.6 mM. UTP, at concentrations up to 2 mM, did not induce depolarization (Figs. 1C and 2A). All measurements were made in the presence of 1 mM Mg^{2+} and in the absence of added Ca^{2+}, to eliminate any direct effects of Ca^{2+} influx on membrane potential. The Hill coefficients generated from these fits were >2.5 for both BzATP and ATP. These values are consistent with previous studies in mast cells (14) and mouse thymocytes (27) and support their conclusion that at least two molecules of ATP (or BzATP) must bind for depolarization to occur.

In contrast, ATP (Fig. 1E) and UTP (Fig. 1F) activated transient increases in $[Ca^{2+}]_i$ in fura-2-loaded BAC1.2F5 macrophages in the absence of extracellular Ca^{2+}, indicative of mobilization of Ca^{2+} from intracellular stores. Nucleotide dose-response curves for peak $[Ca^{2+}]_i$ reached after nucleotide addition showed that ATP and UTP were equipotent in their ability to mobilize intracellular Ca^{2+}, with an estimated EC_{50} of 10 μM and Hill coefficients between 1.0 and 1.25. BzATP, at concentrations up to 1 mM, had no effect on $[Ca^{2+}]_i$ under these conditions (Figs. 1D and 2B).

BzATP-induced depolarization was highly sensitive to extracellular Mg^{2+}. Depolarization in response to 10 μM BzATP was potentiated in the absence of Mg^{2+} (Fig. 3A), suggesting that $BzATP^{4-}$ is the active agonist. Furthermore, BzATP-induced depolarization was reversible upon the addition of 1 mM Mg^{2+}; subsequent chelation of this Mg^{2+} by EDTA was sufficient to reinitiate depolarization (Fig. 3B). Cells depolarized with the ionophore gramicidin, however, were unaffected by additions of Mg^{2+} and EDTA (Fig. 3C), indicating that the effects observed in ATP-depolarized cells are specific to the nucleotide-induced response and not a generalized effect on depolarized cells. The estimated EC_{50} values for BzATP- and ATP-induced depolarization in the absence of Ca^{2+} and Mg^{2+} were shifted to 10 μM and 80 μM, respectively (data not shown). Several studies have suggested UTP^{4-} and ATP^{4-} to be the active ligands for the Ca^{2+}-mobilizing receptor (28–32). However, nucleotide-induced Ca^{2+} mobilization was not sensitive to variations in extracellular Mg^{2+} up to 1 mM. The sensitivity of ATP/BzATP-induced permeabilization to extracellular Mg^{2+} in this range can be used as a discriminating characteristic of the P_{2z} purinoreceptor subtype.

***Xenopus* oocytes injected with BAC1.2F5 poly(A)$^+$ RNA display characteristics of the expression of both the P_{2z} purinoreceptor and the ATP/UTP receptor.** We measured changes in membrane current in voltage-clamped oocytes 2 days after injection of 50 ng of poly(A)$^+$ RNA isolated from BAC1.2F5 macrophages. Two kinetically and pharmacologically distinct responses to extracellular BzATP were detected in RNA-injected oocytes but not in uninjected oocytes. A sustained increase in membrane conductance with a reversal potential of approximately 0 mV was observed in voltage-clamped, BAC1.2F5 poly(A)$^+$ RNA-injected oocytes stimulated with BzATP (Fig. 4B) in the absence of divalent cations, consistent with the activation of an expressed P_{2z}, or pore-forming, purinoreceptor. The expression of this response was highly reproducible and was observed in approximately 98% (53 of 54) of the oocytes injected with BAC1.2F5 poly(A)$^+$ RNA.

The BzATP-induced changes in membrane current were characterized by multiphasic kinetics consisting of three distinct components, 1) an initial rapid increase during the first 5 sec after agonist addition, 2) a plateau or reduced rate of current increase during the next 20–100 sec (depending on BzATP concentration), and 3) a reacceleration of the current increase to a final, steady state rate of increase. Although the magnitude and duration of each phase showed a clear dependence on the concentration of BzATP (Fig. 5), the multiphasic nature of the conductance changes complicated straightforward evaluation

TABLE 1
ATP receptors in phagocytic leukocytes

	Receptor type	
	G protein-coupled	Ligand-gated pore
Cell type	Neutrophils, monocytes, macrophages, and progenitors	Macrophages
Receptor name	P_{2u} purinergic or nucleotide	P_{2z} purinergic
ATP EC_{50} (μM)	10–50	100–500
Agonist selectivity	UTP ≥ ATP ≫ BzATP	BzATP > ATP ≫ UTP
Effects of divalent cations	No major effect	Decrease of potency of nucleotide agonist
Effects on intracellular calcium	Mobilization of intracellular stores	Influx across plasma membrane
Effects on membrane potential	No effect or hyperpolarization (Ca^{2+} dependent)	Depolarization (Ca^{2+} independent)

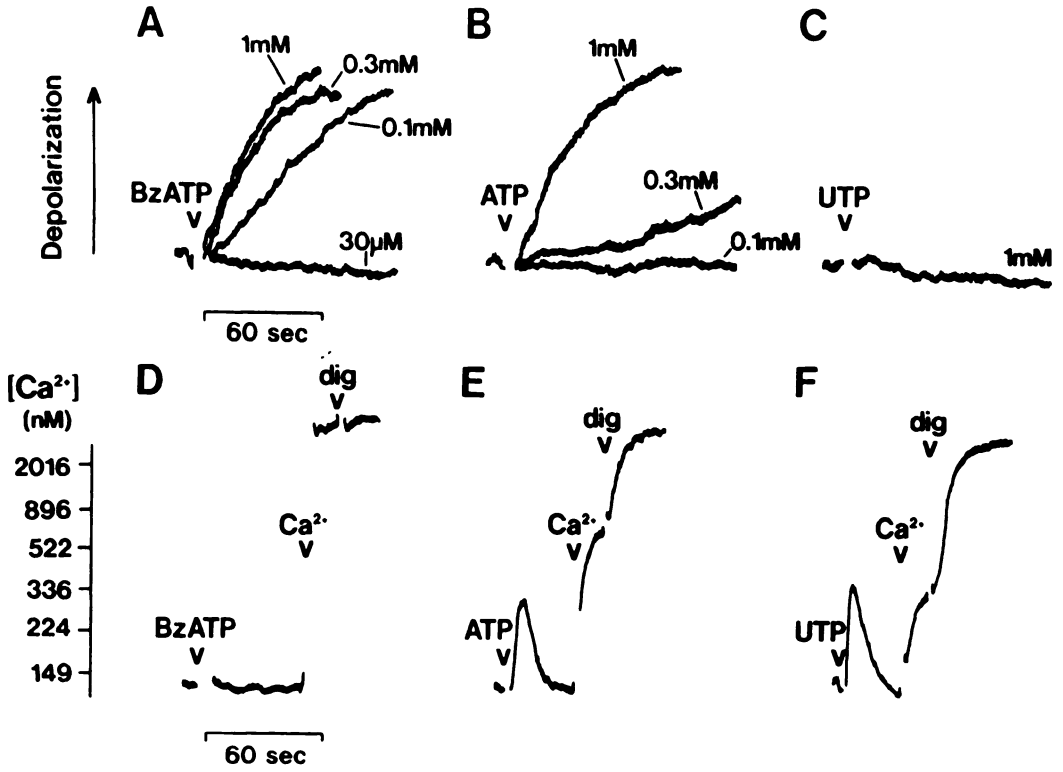

Fig. 1. Effects of extracellular BzATP, ATP, and UTP on membrane potential and $[Ca^{2+}]_i$ in BAC1.2F5 murine macrophages. The membrane potential of BAC1.2F5 cells was measured in the presence of 200 nM bis-oxonol. All measurements were made at a cell concentration of 5×10^5 cells/ml in Ca^{2+}-free BSS supplemented with 5 mM glucose, containing 1 mM Mg^{2+}, at 37°. Cells were stimulated with the indicated concentrations of BzATP (A) or ATP (B) or with 1 mM UTP (C). $[Ca^{2+}]_i$ was measured in fura-2-loaded cells incubated in 37° medium containing (final concentrations) 187 μM Ca^{2+} and 375 μM EGTA (free extracellular Ca^{2+} concentration, 150 nM). These cells (5×10^5 cells/ml) were stimulated with 1 mM BzATP (D), ATP (E), or UTP (F). All data are representative of at least three experiments. dig, digitonin.

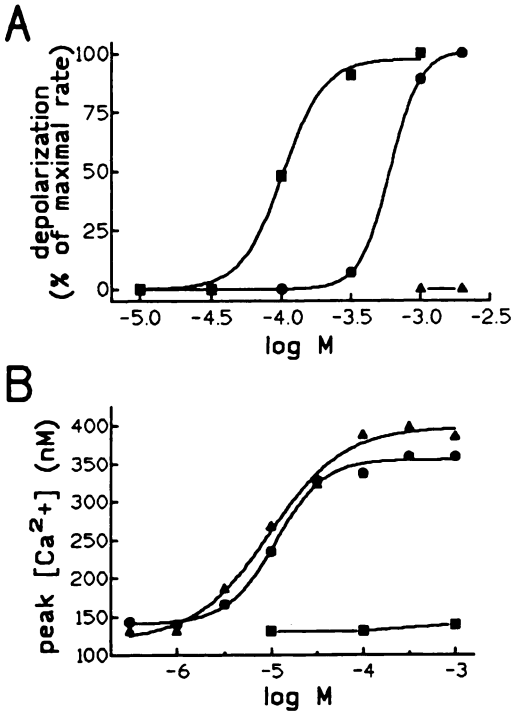

Fig. 2. Nucleotide concentration-response curves describing depolarization (A) and peak $[Ca^{2+}]_i$ changes (B) induced by BzATP (■), ATP (●), and UTP (▲) in BAC1.2F5 macrophages. Experiments were performed under the same conditions as in Fig. 1. Depolarization was defined by the initial rate of depolarization after nucleotide addition, normalized to 100%. Data are representative of at least three independent experiments.

of the concentration-response relationships. Analysis of these time courses indicated that the duration of time between agonist addition and the initiation of the third phase (the final, steady state rate of current increase) was an easily measured parameter that showed a strong inverse dependence on BzATP concentration. Measurement of this parameter also simplified evaluation of the dose-dependent effects of ATP and UTP on the sustained phase of increased membrane current, as opposed to actions of these nucleotides on transient or oscillating changes in membrane current (see below). Nucleotide concentration-response curves describing the effects of BzATP, ATP, and UTP on this parameter of altered membrane conductance in RNA-injected oocytes (Fig. 5B) revealed that BzATP was more potent than ATP; EC_{50} values were 35 μM and 0.3 mM, respectively. The ATP analog ATP[S] also activated the depolarizing current but with an EC_{50} of >1 mM (data not shown). BzATP-induced effects on the sustained current were observed at concentrations as low as 5 μM (Fig. 5A). The corresponding Hill coefficients were between 2.4 and 3.0, consistent with those characterizing the effects of BzATP on depolarization in the BAC1.2F5 macrophages (Fig. 2A). UTP, at concentrations as high as 1 mM, did not activate this sustained current (Figs. 4 and 5).

These poly(A)$^+$ RNA-injected oocytes did respond to UTP (100 μM) with a transient inward current that was followed by current oscillations (Fig. 4, C and D). Similar transient/oscillatory currents were activated in response to 1 μM platelet-activating factor or 100 μM ATP (data not shown). The reversal potential characterizing these UTP-induced currents was approximately −25 mV, consistent with the activation of the

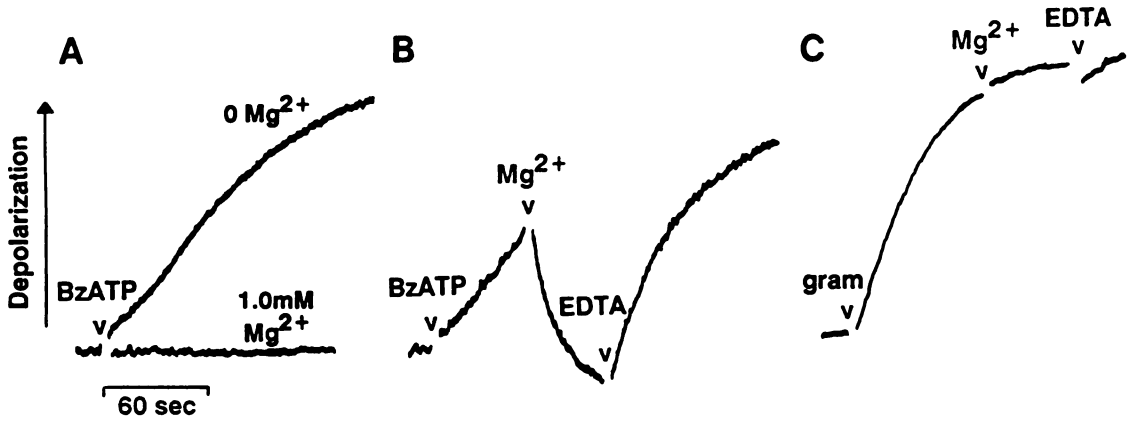

Fig. 3. Effects of Mg^{2+} on BzATP-induced membrane depolarization in BAC1.2F5 macrophages. Membrane potential in BAC1.2F5 cells was measured in the presence of 200 nM bis-oxonol under the same conditions as in Fig. 1. A, Depolarization in response to 10 μM BzATP is shown in the presence or absence of 1 mM Mg^{2+}. B, The addition of 1 mM $MgCl_2$ reversed the depolarization induced by 10 μM BzATP; addition of 2 mM EDTA was sufficient to reinitiate depolarization. C, Depolarization induced by 50 nM gramicidin (*gram*) was unaffected by additions of 2 mM $MgCl_2$ and 4 mM EDTA.

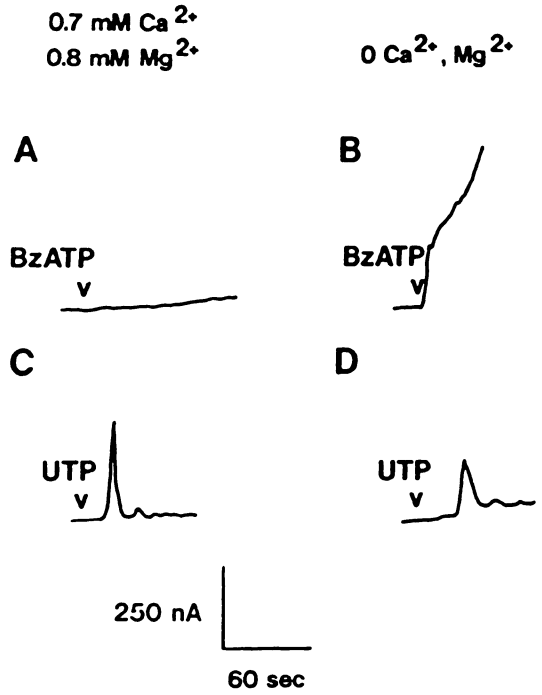

Fig. 4. Expressed nucleotide responsiveness in voltage-clamped *Xenopus* oocytes injected with BAC1.2F5 poly(A)$^+$ RNA. *Xenopus* oocytes were injected with 50 ng of BAC1.2F5 poly(A)$^+$ RNA. After 2 days, single oocytes were voltage-clamped at a holding potential of −60 mV and stimulated with 100 μM BzATP or UTP in MBS with or without divalent cations as indicated. Each pair of additions was performed with oocytes from the same preparation. *Upward traces*, inward currents. Measurements were made at 20°. Each *trace* is representative of the results from at least two independent experiments.

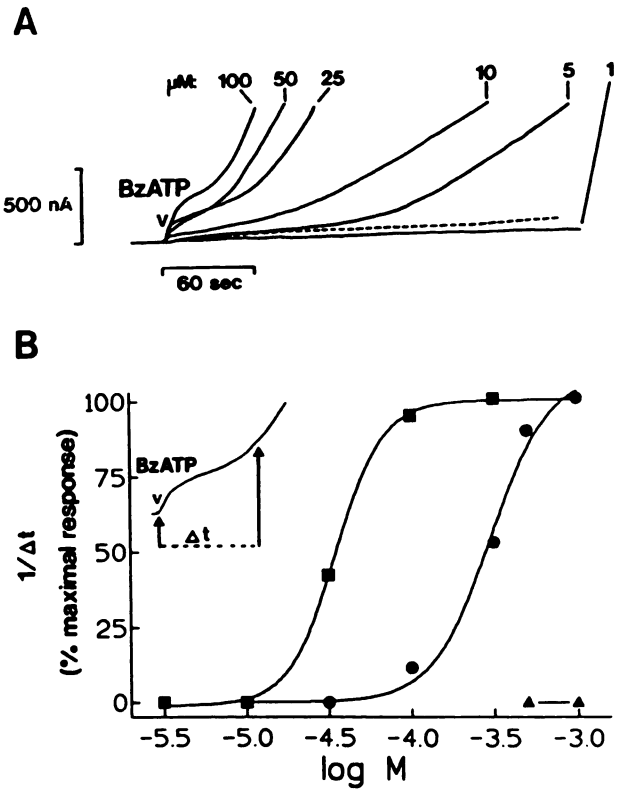

Fig. 5. Concentration-response relationships characterizing the effects of BzATP on membrane current in *Xenopus* oocytes injected with BAC1.2F5 poly(A)$^+$ RNA. A, Oocytes were injected and voltage-clamped as in Fig. 4, in MBS without divalent cations, and were stimulated with the indicated concentrations of BzATP. – – –, Effect of 100 μM BzATP on a control oocyte injected with 50 nl (0.5 ng) of SKR cRNA. B, Nucleotide concentration-response relationships for the effects of BzATP (■), ATP (●), and UTP (▲) on membrane conductance in RNA-injected oocytes. The *y*-axis plots the inverse of the time interval between agonist addition and peak sustained rate of change in membrane current; the inverse times observed with different concentrations of BzATP/ATP/UTP have been normalized to the maximal inverse time interval measured in oocytes stimulated with 300 μM BzATP. These data, obtained using a single batch of injected oocytes, are representative of four independent experiments using separate batchs of injected oocytes.

endogenous Ca^{2+}-activated Cl^- channel (33, 34). Expression efficiency varied between frogs and experiments. In general, peak currents ranged from 30 to 250 nA and were observed in approximately 80% (22 of 28) of the mRNA-injected oocytes. None of the tested nucleotides induced changes in membrane current, either sustained nor transient, in control oocytes injected with water or with 50 ng of cRNA encoding the SKR (0 of 10 oocytes). Moreover, in oocytes injected with mRNA isolated from other cells that express the Ca^{2+}-mobilizing nucleotide receptor but not the pore-forming P_{2z}-type purinoreceptor, only the ATP/UTP-induced transient currents were

observed. These included the HL-60 leukocyte cell line (35), the DDT_1MF-2 smooth muscle cell line (36), and human amnion cells (37) (data not shown).

The effects of extracellular nucleotides on $[Ca^{2+}]_i$ in oocytes were also addressed, using aequorin as an indicator of changes in $[Ca^{2+}]_i$. Oocytes coinjected with BAC1.2F5 poly(A)$^+$ RNA and aequorin displayed transient increases in aequorin luminescence in response to ATP, UTP, ADP, and ATP[S] (Fig. 6). These responses were independent of extracellular Ca^{2+}, which indicated that the increases in luminescence resulted from the release of Ca^{2+} from intracellular stores. Increases in aequorin luminescence were not observed either in control uninjected oocytes stimulated with UTP (Fig. 6F) or in RNA-injected oocytes stimulated with 0.01–1 mM BzATP (Fig. 6A). Thus, whereas BzATP acts as a potent and efficacious agonist for activating the sustained membrane current, it is ineffective as a Ca^{2+}-mobilizing agonist.

BzATP-induced currents were attenuated in the presence of divalent cations (0.7 mM Ca^{2+}, 0.8 mM Mg^{2+}) (Figs. 4A and 7B). BzATP-induced changes in membrane conductance were reversed upon the addition of a 20-fold molar excess of Mg^{2+} over BzATP and were reinitiated after the chelation of the Mg^{2+} ions with EDTA (Fig. 7A). This phenomenon was similar to the reversible changes in membrane potential observed in BzATP-stimulated BAC1.2F5 cells (Fig. 3B). EDTA at 2 mM activated the sustained membrane current when BAC1.2F5 poly(A)$^+$ RNA-injected oocytes were incubated in the presence of 1 mM $MgCl_2$ and 50 μM BzATP (Fig. 7B). In the absence of BzATP, however, 2 mM EDTA did not elicit this response, suggesting that the effects of EDTA were due to the chelation of Mg^{2+} and the generation of the $BzATP^{4-}$ species.

mRNA(s) encoding the P_{2z}-type purinoreceptor and Ca^{2+}-mobilizing nucleotide receptor are enriched in a 2.5–4.0 kb fraction. Poly(A)$^+$ RNA isolated from BAC1.2F5 cells was size fractionated and pooled as described in Experimental Procedures. Injection of 50 ng of poly(A)$^+$ RNA from these pools into *Xenopus* oocytes revealed an enrichment of both BzATP-induced sustained currents and UTP-induced transient currents in a fraction enhanced in poly(A)$^+$ RNA in the 2.5–4.0-kb range (Fig. 8). This fraction contained approximately 20% of the total RNA eluted from the gradient. The P_{2z} purinoreceptor-induced response was also observed in oocytes injected with poly(A)$^+$ RNA from fractions containing species of ≥3.0 kb. This suggests that the RNA species encoding these receptors are in the 3.0–4.0-kb size range. Conversely, UTP-dependent transient currents were also detected in oocytes injected with poly(A)$^+$ RNA from a fraction enriched in 1.0–3.0-kb species, suggesting that the mRNA species encoding this receptor subtype are in the 2.0–3.0-kb size range.

Discussion

We have demonstrated for the first time the expression of an exogenous pore-forming P_{2z} purinoreceptor in *Xenopus* oocytes injected with macrophage poly(A)$^+$ RNA. BzATP and ATP activated a sustained depolarization in the native BAC1.2F5 macrophages and a kinetically similar increase in membrane conductance in poly(A)$^+$ RNA-injected, voltage-clamped oocytes. The specificity of these latter responses for ATP^{4-} is consistent with the expression of a pore-forming, P_{2z}-type purinoreceptor. Ca^{2+}-mobilizing nucleotide receptors, encoded by macrophage-derived mRNA, were also expressed in the poly(A)$^+$ RNA-injected oocytes. UTP and ATP, but not BzATP, activated mobilization of intracellular Ca^{2+} stores in BAC1.2F5 macrophages. In a similar manner, ATP and UTP, but not BzATP, produced transient increases in $[Ca^{2+}]_i$, as indicated by both aequorin luminescence and the activation of

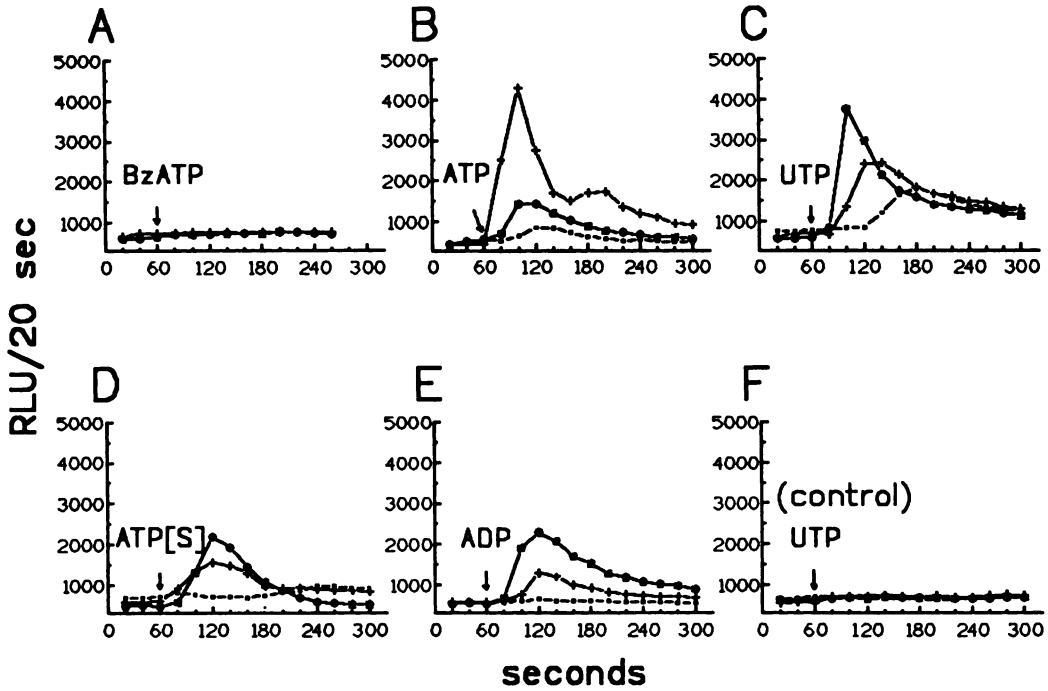

Fig. 6. Nucleotide-dependent effects on aequorin luminescence in oocytes injected with BAC1.2F5 poly(A)$^+$ RNA. Oocytes were injected with 12 ng of aequorin 3 days after RNA injections. Luminescence was recorded from individual oocytes, in relative light units (*RLU*) integrated over 20-sec intervals. Nucleotides were added as indicated, at concentrations of 1 mM (*), 0.1 mM (+), and 10 μM (■). All measurements were made at 20° and are representative of at least two experiments. *A-E*, experiments wherein oocytes were injected with macrophage mRNA; *F*, experiments wherein oocytes were not injected with mRNA.

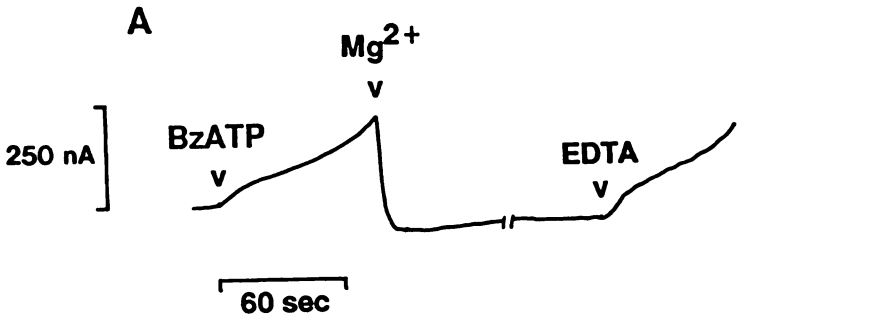

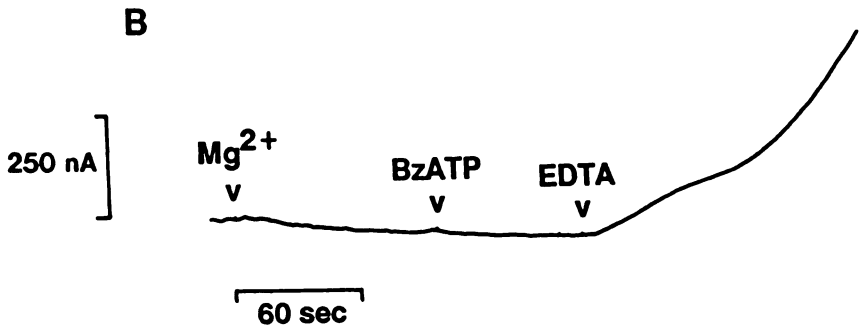

Fig. 7. Effects of Mg^{2+} on BzATP-induced membrane current in *Xenopus* oocytes injected with BAC1.2F5 poly(A)$^+$ RNA. Oocytes were injected and voltage-clamped as described for Fig. 4, in MBS without divalent cations. A, An oocyte was stimulated with 50 μM BzATP; 1 mM $MgCl_2$ and 2 mM EDTA were added as indicated. B, An oocyte was stimulated with 50 μM BzATP after the addition of 1 mM Mg^{2+}; the response was initiated upon the addition of 2 mM EDTA as indicated. Results are representative of at least two independent experiments.

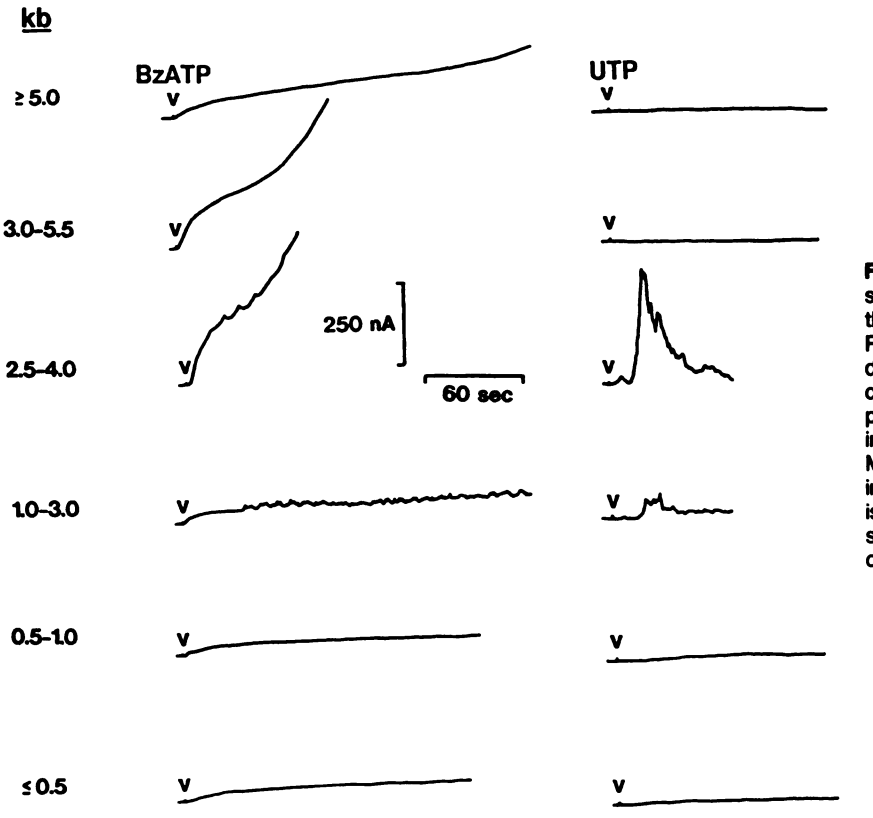

Fig. 8. Enrichment by sucrose fractionation of mRNA species encoding the BAC1.2F5 P_{2z} purinoreceptor and the Ca^{2+}-mobilizing nucleotide receptor. Total poly(A)$^+$ RNA isolated from BAC1.2F5 cells was fractionated as described in Experimental Procedures. *Xenopus* oocytes were injected with 50 ng of the fractionated poly(A)$^+$ RNA and voltage-clamped as in Fig. 4. RNA-injected oocytes were stimulated with 50 μM BzATP in MBS without divalent cations (*left*) or with 100 μM UTP in MBS (*right*). The size range of RNA in each fraction is indicated at the *far left*. Data were obtained from a single experiment and are representative of three independent experiments.

transient/oscillatory inward currents, in the RNA-injected oocytes. These latter responses were independent of extracellular Ca^{2+} and presumably resulted from the mobilization of intracellular Ca^{2+} stores and subsequent activation of the Ca^{2+}-dependent Cl^- channels endogenously expressed in these oocytes.

The lack of discriminating antagonists has hampered the direct identification of proteins that constitute the various P_2 purinoreceptor subtypes. Thus, *Xenopus* oocytes provide a useful tool for the characterization of the mRNA species that encode the receptor proteins. Two laboratories have used this system to express and characterize G protein-coupled, Ca^{2+}-mobilizing, P_2-type purinoreceptors. Murphy and Tiffany (23) described the expression of an ATP[S]/UTP-induced $^{45}Ca^{2+}$ efflux in oocytes injected with poly(A)$^+$ RNA isolated from differentiated HL-60 human granulocytes. Similarly, Honore *et al.* (24) showed that ATP and UTP stimulate a Ca^{2+}-activated Cl^- current in oocytes injected with poly(A)$^+$ RNA from fetal

guinea pig brain and then depolarized from −100 mV to 20 mV. The transient ATP/UTP-induced responses characterized in these earlier expression studies are functionally and pharmacologically distinct from the sustained BzATP-induced responses observed in BAC1.2F5 macrophages and in BAC1.2F5 poly(A)$^+$ RNA-injected oocytes. In addition, the agonist selectivity for the nucleotide-induced transient increases in $[Ca^{2+}]_i$ described previously and in this paper includes a variety of adenine nucleotides as well as UTP. Nucleotide-induced sustained Ca^{2+} influx and depolarization, in contrast, are activated only by ATP, BzATP, and to a lesser extent ATP[S] and are sensitive to extracellular divalent cations. These differences strongly suggest that the BzATP-selective responses observed in BAC1.2F5 poly(A)$^+$ RNA-injected oocytes result from the expression of a purinoreceptor that is distinct from those previously expressed in *Xenopus* oocytes.

Fractionation of BAC1.2F5 macrophage poly(A)$^+$ RNA enriched the mRNA species encoding the components of both the pore-forming P_{2z}-type purinoreceptor and the Ca^{2+}-mobilizing nucleotide receptor in a fraction containing RNA in the 2.5–4.0-kb size range (Fig. 8). This is consistent with the size range of mRNA species encoding other G protein-coupled, Ca^{2+}-mobilizing receptors and suggests that the Ca^{2+}-mobilizing nucleotide receptor may be similarly composed of a single polypeptide (38). The pore-forming P_{2z}-type purinoreceptor, which is functionally similar to the family of receptor ion channels, is likely to exist as an oligomeric complex, as either a hetero-oligomer or a homo-oligomer. It will be important to determine how many unique polypeptides constitute functional P_{2z}-type purinoreceptors.

BzATP was initially developed as a photoaffinity probe for the labeling of the nucleotide binding site on F_1-ATPase (39). It was subsequently identified as an agonist for a subset of the P_2 purinoreceptors, including P_{2y} (40) and P_{2z} (41). Photoincorporated BzATP has been shown to activate early mitogenic responses in 3T3, 3T6, and A-431 cells (42) and to promote GTP[S] activation of phospholipase C in turkey erythrocyte membranes (40). The putative labeling of the P_{2y} purinoreceptor on turkey erythrocyte membranes was subsequently demonstrated using [^{32}P]BzATP as a photoaffinity probe (43). Based on its potency and specificity for the P_{2z} purinoreceptor-induced responses in macrophages, BzATP may be used as a photoaffinity probe for identifying putative P_{2z} purinoreceptor proteins in these cells.

The specific characteristics of ATP-induced permeabilization vary in different cell types. P_{2z} purinoreceptor-mediated responses fall into two broad catagories. In all cells expressing this receptor subtype, ATP activates a generalized increase in cation permeability that is characterized by enhanced Ca^{2+} and Na^+ influx and depolarization. In some cell types, such as transformed fibroblasts (7), mast cells (8, 9), and macrophages (5), ATP, acting through the P_{2z} purinoreceptor, induces an increased permeability to molecules of ≤900 Da. In other cell types, however, P_{2z} purinoreceptor-dependent permeability is limited to smaller molecules (44–46). In CLL lymphocytes, for example, ATP increases membrane permeability to the fluorescent cation ethidium (314 Da) but not to propidium (414 Da).[1] The selectivity for BzATP, ATP, and ATP[S], the requirement for a relatively high concentration of agonist, and the sensitivity to divalent cations suggest that these responses result from the activation of the same or similar receptors.

The size of ATP-induced pores in a given cell type appears to vary with ATP concentration. Cockroft and Gomperts (9) reported a consistent loss of inorganic phosphate from mast cells in response to 1.4 μM ATP^{4-}, whereas 8.6 μM ATP^{4-} increased cell permeability to phosphorylated metabolites and nucleotides, in addition to inorganic phosphate. In other studies in mast cells, Tatham and Lindau (14) examined the effects of increasing ATP^{4-} concentrations on Ca^{2+}/GTP-dependent exocytosis. At relatively low concentrations of ATP^{4-} (2.5–5 μM), mast cells became permeant to Ca^{2+}, resulting in the activation of exocytosis. At higher concentrations of ATP^{4-}, the cells also became permeant to larger molecules, including GTP. At these ATP^{4-} concentrations, exocytosis was not observed, presumably due to the loss of GTP from the cytosol. Only when GTP[S] was provided in the extracellular medium did exocytosis take place. Furthermore, patch-clamp studies in both mast cells (14) and macrophages (47) revealed a wide variation in the unit conductance of these pores. These observations suggest that ATP-dependent pores exist as a heterologous population and that their size varies with ATP concentration. This is consistent with our observations that the rate and magnitude of the P_{2z} purinoreceptor-mediated Ca^{2+} influx and depolarization in BAC1.2F5 cells and oocytes injected with BAC1.2F5 poly(A)$^+$ RNA are dependent on the concentration of BzATP.

Variations in pore size and rate of permeabilization have raised the possibility that additional receptor monomers are recruited to form the larger pores in response to increasing concentrations of ATP^{4-}. If this is the case, then cell-specific variations in P_{2z} purinoreceptor-induced permeabilization may reflect variable levels of receptor protein expression. Our data from the sucrose fractionation of BAC1.2F5 RNA are consistent with this possibility. Oocytes injected with the same amount of RNA from fractions containing 2.5–4.0-, 3.0–5.0-, and ≥5.0-kb RNA all exhibited BzATP-induced increases in membrane current. However, the rate of this increase in response to the same concentration of BzATP was markedly slower in oocytes injected with ≥5.0-kb RNA, compared with oocytes injected with 2.5–4.0-kb RNA. This difference may reflect the relative abundance of P_{2z} purinoreceptor mRNA in these pools and, thus, the relative number of receptors expressed in RNA-injected oocytes. In addition, oocytes injected with the same amount of total BAC1.2F5 poly(A)$^+$ RNA in a given experiment displayed a faster onset of the BzATP-induced sustained current when assayed 2 days versus 1 day after injection.[2] This suggests that the increased rate of the BzATP-induced response may be correlated with the relative expression level of exogenous macrophage proteins.

Alternatively, variations in P_{2z} purinoreceptor-induced permeabilization may reflect the presence or absence of accessory proteins involved in pore formation. Beyer and Steinberg (48) have reported that loss of ATP-induced permeabilization in a mutant of the J774 macrophage cell line can be correlated with the greatly reduced expression of connexin-43 mRNA and protein. These data suggest that this gap junction protein may play a role in ATP-induced pore formation. The oocyte expression system can be used to directly address the potential interaction of the P_{2z} purinoreceptor with additional proteins that may be involved in the formation of these ATP-induced pores.

[1] James Wiley, personal communication.

[2] L. Nuttle and G. Dubyak, unpublished observations.

References

1. Gordon, J. L. Extracellular ATP: effects, sources and fate. *Biochem. J.* **233**:309–319 (1986).
2. Dubyak, G. R. Signal transduction by P_2-purinergic receptors for extracellular ATP. *Am. J. Respir. Cell Mol. Biol.* **4**:295–300 (1991).
3. El-Moatassim, C., J. Dornand, and J. C. Mani. Extracellular ATP and cell signalling. *Biochim. Biophys. Acta* **1134**:31–45 (1992).
4. Sung, S. S. J., J. D. E. Young, A. M. Origlio, J. M. Heiple, H. R. Kaback, and S. C. Silverstein. Extracellular ATP perturbs transmembrane ion fluxes, elevates cytosolic [Ca^{2+}], and inhibits phagocytosis in mouse macrophages. *J. Biol. Chem.* **260**:13442–13449 (1985).
5. Steinberg, T. H., A. S. Newman, J. A. Swanson, and S. C. Silverstein. ATP^{4-} permeabilizes the plasma membrane of mouse macrophages to fluorescent dyes. *J. Biol. Chem.* **262**:8884–8888 (1987).
6. Greenberg, S., F. Di Virgilio, T. H. Steinberg, and S. C. Silverstein. Extracellular nucleotides mediate Ca^{2+} fluxes in J774 macrophages by two distinct mechanisms. *J. Biol. Chem.* **263**:10337–10343 (1988).
7. Rozengurt, E., and L. A. Heppel. A specific effect of external ATP on the permeability of transformed 3T3 cells. *Biochem. Biophys. Res. Commun.* **67**:1581–1588 (1975).
8. Dahlquist, R. Relationship of uptake of sodium and ^{45}calcium to ATP-induced histamine release in rat mast cells. *Acta Pharmacol. Toxicol.* **35**:11–22 (1974).
9. Cockcroft, S., and B. D. Gomperts. ATP induces nucleotide permeability in rat mast cells. *Nature (Lond.)* **279**:541–542 (1979).
10. Di Virgilio, F., V. Bronte, D. Collavo, and P. Zanovello. Responses of mouse lymphocytes to extracellular adenosine 5′-triphosphate (ATP): lymphocytes with cytotoxic activity are resistant to the permeabilizing effects of ATP. *J. Immunol.* **143**:1955–1960 (1989).
11. El-Moatassim, C., T. Maurice, J. C. Mani, and J. Dornand. The intracellular calcium concentration increase induced in murine thymocytes by extracellular ATP does not involve ATP hydrolysis and is not related to phosphoinositide metabolism. *FEBS Lett.* **242**:391–396 (1989).
12. Whetton, A. D., S. J. Huang, and P. N. Monk. Adenosine triphosphate can maintain multipotent hemopoietic stem cells in the absence of interleukin 3 via a membrane permeabilization mechanism. *Biochem. Biophys. Res. Commun.* **152**:1173–1178 (1988).
13. Di Virgilio, F., C. Fasolato, and T. H. Steinberg. Inhibitors of membrane transport system for organic anions block fura-2 excretion from PC12 and N2A cells. *Biochem. J.* **256**:959–963 (1988).
14. Tatham, P. E. R., and M. Lindau. ATP-induced pore formation in the plasma membrane of rat peritoneal mast cells. *J. Gen. Physiol.* **95**:459–476 (1990).
15. Rozengurt, E., L. A. Heppel, and I. Friedberg. Effect of exogenous ATP on the permeability properties of transformed cultures of mouse cell lines. *J. Biol. Chem.* **252**:4584–4590 (1977).
16. Rozengurt, E., and L. A. Heppel. Reciprocal control of membrane permeability of transformed cultures of mouse cell lines by external and internal ATP. *J. Biol. Chem.* **254**:708–714 (1979).
17. Gomperts, B. D. Involvement of guanine nucleotide-binding protein in the gating of Ca^{2+} by receptors. *Nature (Lond.)* **306**:64–66 (1983).
18. Blanchard, D. K., S. McMillen, and J. Y. Djeu. γ-Interferon enhances sensitivity of human macrophages to extracellular ATP-mediated lysis. *J. Immunol.* **147**:2579–2585 (1991).
19. Zheng, L. M., A. Zychlinsky, C. C. Liu, D. M. Ojcius, and J. D. E. Young. Extracellular ATP as a trigger for apoptosis or programmed cell death. *J. Cell. Biol.* **112**:279–288 (1991).
20. El-Moatassim, C., and G. R. Dubyak. A novel pathway for the activation of phospholipase D by P_{2z} purinergic receptors in BAC1.2F5 macrophages. *J. Biol. Chem.* **267**:23664–23673 (1992).
21. Steinberg, T. H., and F. Di Virgilio. Cell-mediated cytotoxicity: ATP as an effector and the role of target cells. *Curr. Opin. Immunol.* **3**:711–715 (1991).
22. Fillipini, A., R. E. Taffs, and M. V. Sitkovsky. Extracellular ATP in T-lymphocyte activation: possible role in effector functions. *Proc. Natl. Acad. Sci. USA* **87**:8267–8271 (1990).
23. Murphy, P. M., and H. L. Tiffany. Characterization of phagocyte P_2 nucleotide receptors expressed in *Xenopus* oocytes. *J. Biol. Chem.* **265**:11615–11621 (1990).
24. Honore, E., F. Fournier, T. Collin, J. Nargeot, and P. Guilbault. Functional expression of P_{2y} purinoceptor in *Xenopus* oocytes injected with brain mRNA. *Eur. J. Physiol.* **418**:447–452 (1991).
25. Rink, T. J., C. Montecucco, T. R. Hesketh, and R. Y. Tsien. Lymphocyte membrane potential assessed with fluorescent probes. *Biochim. Biophys. Acta* **595**:15–30 (1980).
26. Chomczynski, P., and N. Sacchi. Single-step method of RNA isolation by acid guanidinium thiocyanate-phenol-chloroform extraction. *Anal. Biochem.* **162**:156–159 (1987).
27. Pizzo, P., P. Zanovello, V. Bronte, and F. Di Virgilio. Extracellular ATP causes lysis of mouse thymocytes and activates a plasma membrane ion channel. *Biochem. J.* **274**:139–144 (1991).
28. Tawada, Y., K. I. Furukawa, and M. Shigekawa. ATP-induced calcium transient in cultured rat aortic smooth muscle cells. *J. Biochem. (Tokyo)* **102**:1499–1509 (1987).
29. Fine, J., P. Cole, and J. S. Davidson. Extracellular nucleotides stimulate receptor-mediated calcium mobilization and inositol phosphate production in human fibroblasts. *Biochem. J.* **263**:371–376 (1989).
30. Davidson, J. S., I. K. Wakefield, U. Sohnius, A. P. Van Der Merwe, and R. P. Millar. A novel extracellular nucleotide receptor coupled to phosphoinositidase C in pituitary cells. *Endocrinology* **126**:80–87 (1990).
31. Brown, H. A., E. R. Lazarowski, R. C. Boucher, and T. K. Harden. Evidence that UTP and ATP regulate phospholipase C through a common nucleotide receptor in human airway epithelial cells. *Mol. Pharmacol.* **40**:648–655 (1991).
32. Lustig, K. D., M. G. Sportiello, L. Erb, and G. A. Weisman. A nucleotide receptor in vascular endothelial cells is specifically activated by the fully ionized forms of ATP and UTP. *Biochem. J.* **284**:733–739 (1992).
33. Oron, Y., N. Dascal, E. Nadler, and M. Lupu. Inositol 1,4,5-triphosphate mimics muscarinic response in *Xenopus* oocytes. *Nature (Lond.)* **313**:141–143 (1985).
34. Takahashi, T., E. Neher, and B. Sakmann. Rat brain serotonin receptors in *Xenopus* oocytes are coupled by intracellular calcium to endogenous channels. *Proc. Natl. Acad. Sci. USA* **84**:5063–5067 (1987).
35. Dubyak, G. R., D. S. Cowen, and L. M. Meuller. Activation of inositol phospholipid breakdown in HL-60 cells by P_2-purinergic receptors for extracellular ATP. *J. Biol. Chem.* **263**:18108–18117 (1988).
36. Gerwins, P., and B. B. Fredholm. ATP and its metabolite adenosine act synergistically to mobilize intracellular calcium via the formation of inositol 1,4,5-triphosphate in a smooth muscle cell line. *J. Biol. Chem.* **267**:16081–16087 (1992).
37. Vander Kooy, D., G. R. Dubyak, R. M. Moore, and J. J. Moore. Adenosine triphosphate activates the phospholipase-C cascade system in human amnion cells without increasing prostaglandin production. *Endocrinology* **124**:2005–2012 (1989).
38. Dohlman, H. G., J. Thorner, M. G. Caron, and R. J. Lefkowitz. Model systems for the study of seven-transmembrane segement receptors. *Annu. Rev. Biochem.* **60**:653–688 (1991).
39. Williams, N., and P. S. Coleman. Exploring the adenine-nucleotide binding sites on mitochondrial F_1-ATPase with a new photoaffinity probe, 3′-*O*-(4-benzoyl)benzoyl adenosine 5′-triphosphate. *J. Biol. Chem.* **257**:2834–2841 (1982).
40. Boyer, J. L., and T. K. Harden. Irreversible activation of phospholipase C-coupled P_{2y} purinergic receptors by 3′-*O*-(4-benzoyl)benzoyl adenosine 5′-triphosphate. *Mol. Pharmacol.* **36**:381–385 (1989).
41. Gonzalez, F. A., A. H. Ahmed, K. D. Lustig, L. Erb, and G. A. Weisman. Permeabilization of transformed mouse fibroblasts by 3′-*O*-(4-benzoyl)benzoyl adenosine 5′-triphosphate and the desensitization of the process. *J. Cell. Physiol.* **139**:109–115 (1989).
42. Gonzalez, F. A., D. Wang, N.-H. Huang, and L. A. Heppel. Activation of early event of the mitogenic response by a P_{2y} purinoceptor with covalently bound 3′-*O*-(4-benzoyl)benzoyl adenosine 5′-triphosphate. *Proc. Natl. Acad. Sci. USA* **87**:9717–9721 (1990).
43. Boyer, J. L., C. L. Cooper, and T. K. Harden. [^{32}P]-3′-*O*-(4-Benzoyl)benzoyl ATP as a photoaffinity label for a phospholipase C-coupled P_{2y} purinergic receptor. *J. Biol. Chem.* **265**:13515–13520 (1990).
44. Wiley, J. S., and G. R. Dubyak. Extracellular adenosine triphosphate increases cation permeability of chronic lymphocytic leukemic lymphocytes. *Blood* **73**:1316–1323 (1989).
45. El Moatassim, C., J. C. Mani, and J. Dornand. Extracellular ATP^{4-} permeabilizes thymocyte plasma membranes not only to cations but also to low molecular weight solutes. *Eur. J. Pharmacol.* **18**:111–118 (1990).
46. Soltoff, S. P., M. K. McMillian, and B. R. Talamo. ATP activates a cation-permeable pathway in rat parotid acinar cells. *Am. J. Physiol.* **262**:C934-C940 (1992).
47. Buisman, H. P., T. H. Steinberg, J. Fischbarg, S. C. Silverstein, S. A. Vogelzang, C. Ince, D. L. Ypey, and P. C. J. Leijh. Extracellular ATP induces a large nonselective conductance in macrophage plasma membranes. *Proc. Natl. Acad. Sci. USA* **85**:7988–7992 (1988).
48. Beyer, E. C., and T. H. Steinberg. Evidence that the gap junction protein connexin-43 is the ATP-induced pore of mouse macrophages. *J. Biol. Chem.* **266**:7971–7974 (1991).

Send reprint requests to: Louise C. Nuttle, Department of Physiology and Biophysics, School of Medicine, Case Western Reserve University, Cleveland, OH 44106.